

Supporting Information

Sequential molecular doping of non-fullerene organic solar cells without hole transport layers

Dongyang Zhang,^a Jianqiu Wang,^{ab} Xuning Zhang,^a Jiyu Zhou,^a Saud-uz-Zafar,^b Huiqiong Zhou,^b Yuan Zhang^{*a}

^a School of Chemistry
Beijing Advanced Innovation Center for Biomedical Engineering
Beihang University
No. 37 Xueyuan Road, Beijing 100191, P. R. China
E-mail: yuanzhang@buaa.edu.cn

^b Key Laboratory of Nanosystem and Hierarchical Fabrication
CAS Center for Excellence in Nanoscience,
National Center for Nanoscience and Technology
Beijing 100190, P. R. China
E-mail: zhouhq@nanoctr.cn

Table S1. Photovoltaic parameters of best PBDB-T:ITIC solar cells at different doping conditions.

Doping method	HTL	Doping condition	V_{oc} (V)	J_{sc} (mA/cm ²)	FF (%)	PCE (%)
Bulk doping	MoO _x	0%	0.89	16.61	67.71	10.01
		0.1%	0.89	16.10	67.90	9.73
		0.2%	0.89	15.67	65.17	9.09
Sequential doping	MoO _x	30 s	0.89	16.83	71.16	10.66
	w/o	w/o	0.16	12.67	42.09	0.85
		0 s	0.87	16.28	64.24	9.10
		20 s	0.87	16.00	68.34	9.51
		40 s	0.87	17.01	67.34	9.97
		60 s	0.87	16.78	65.20	9.52
		80 s	0.87	16.06	64.96	9.07

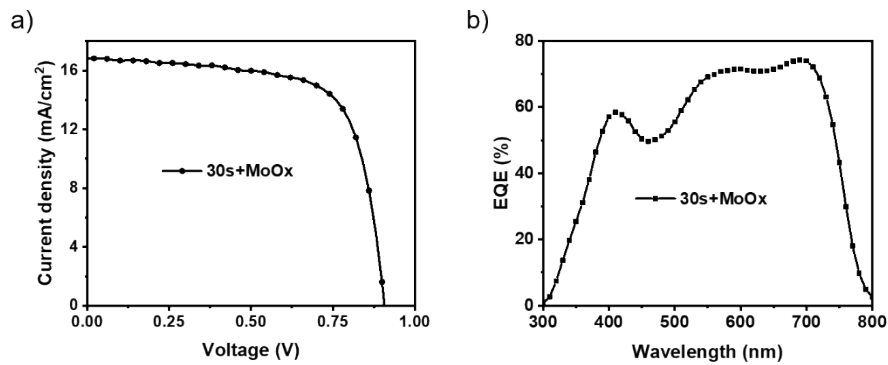


Figure S1. (a) Current density versus voltage (J-V) characteristics of sequential molecular doping device with MoO_x after 30s penetration under AM 1.5 G solar irradiation. (b) EQE spectra of sequentially doped PBDBT:ITIC solar cells with MoO_x after 30s penetration.

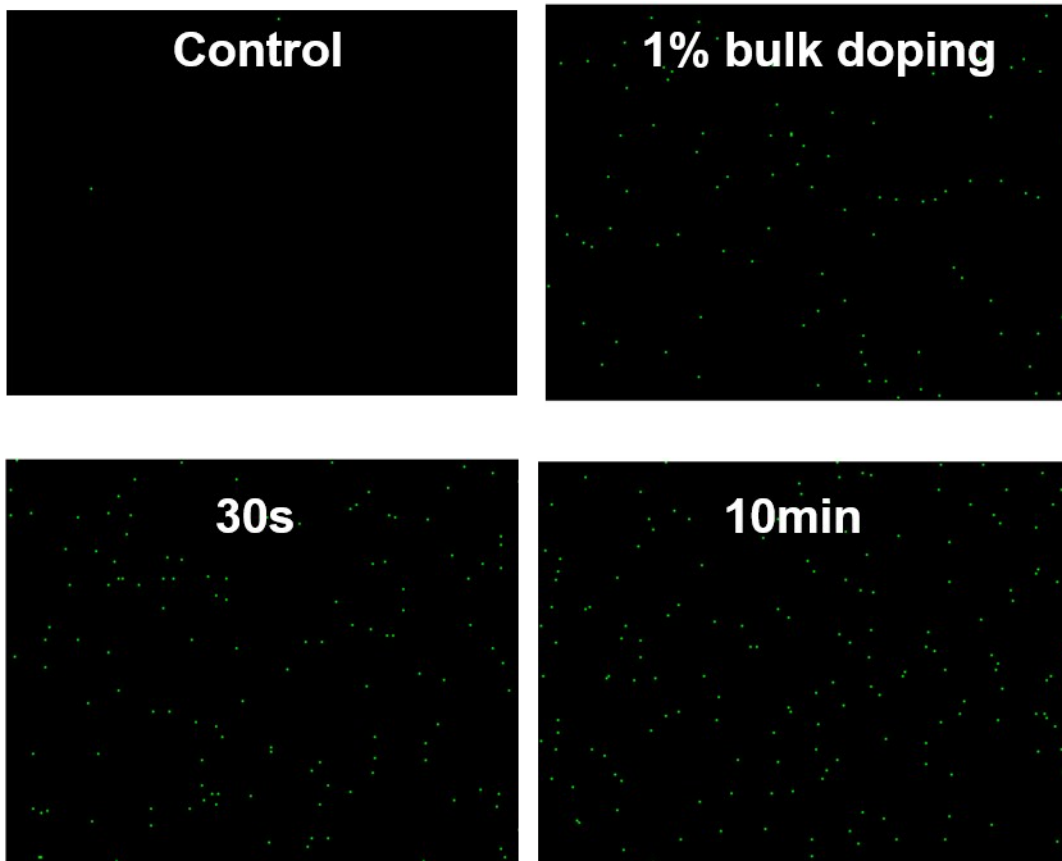


Figure S2. Elemental mapping of fluorine based on EDX analysis of PBDB-T:ITIC BHJ films with different doping methods.

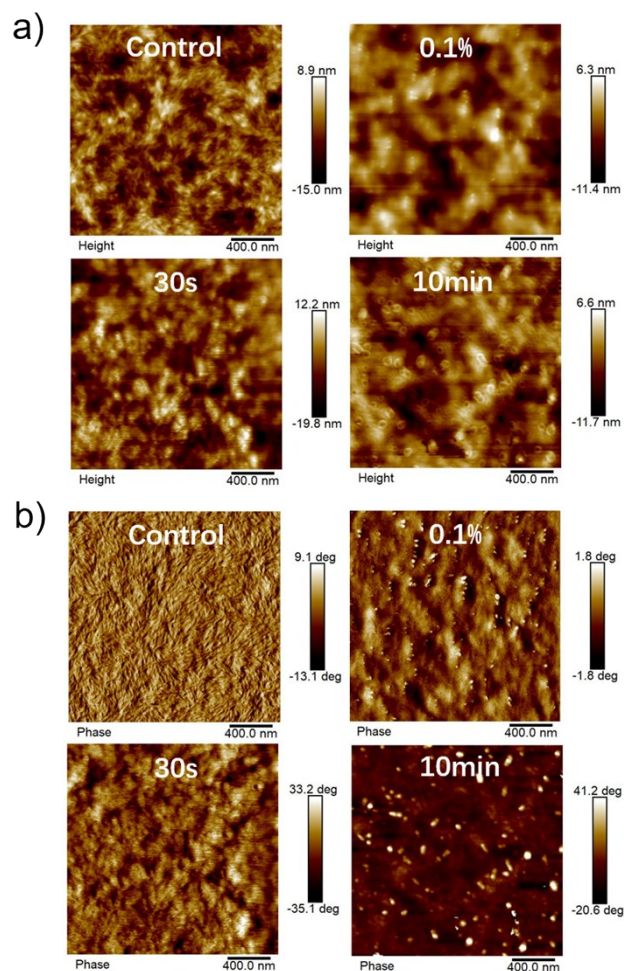


Figure S3. (a) Topographic and (b) phase images of pristine, bulk doped (0.1%) and sequentially doped (30 s and 10 min) PBDB-T:ITIC BHJ films.

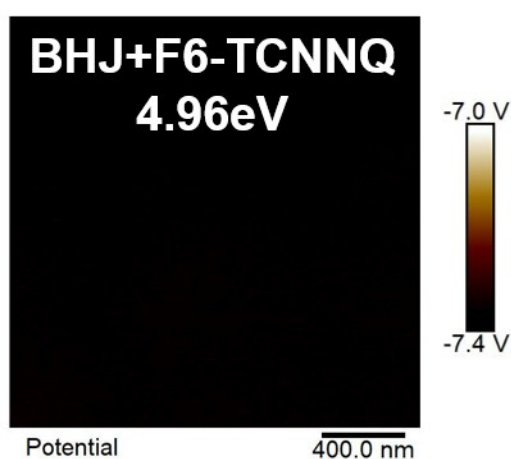


Figure S4. 2D mapping of the surface potential attained by scanning Kelvin probe microscopy for BHJ film spun-coat with F6-TCNNQ solution (conc. = 1.5 mg/mL).

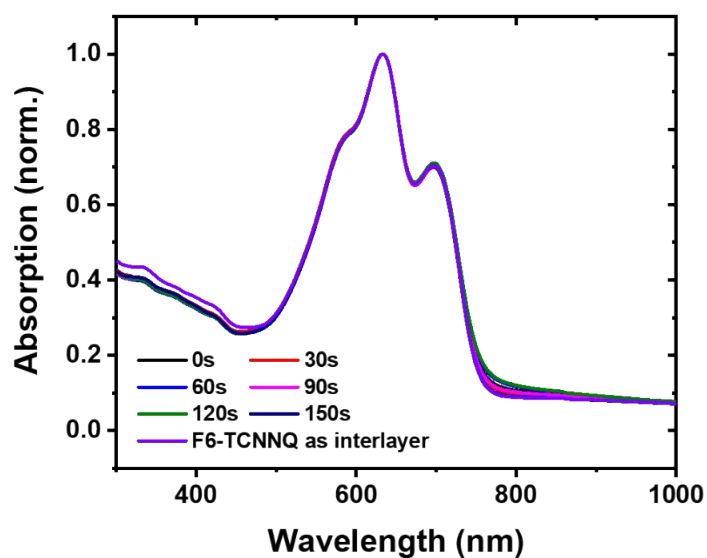


Figure S5. Absorption spectra of PBDB-T:ITIC BHJ films in different sequential doping conditions.

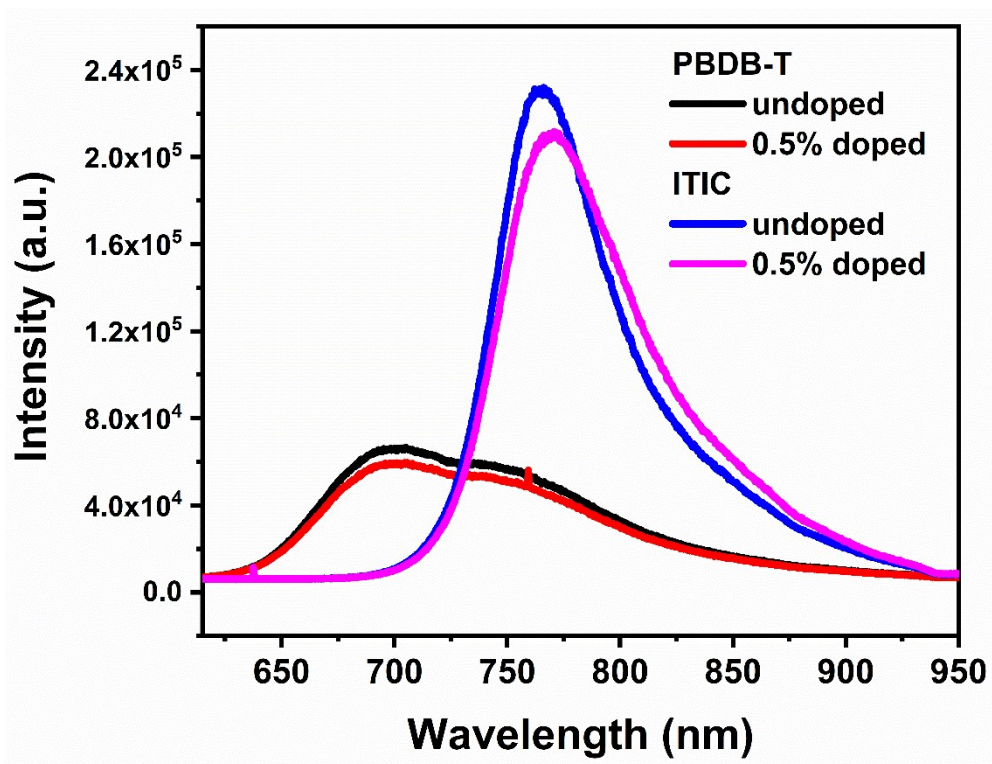


Figure S6. Steady-state photoluminescence (PL) spectra of undoped and F6-TCNNQ doped PBDB-T or ITIC films in different conditions.

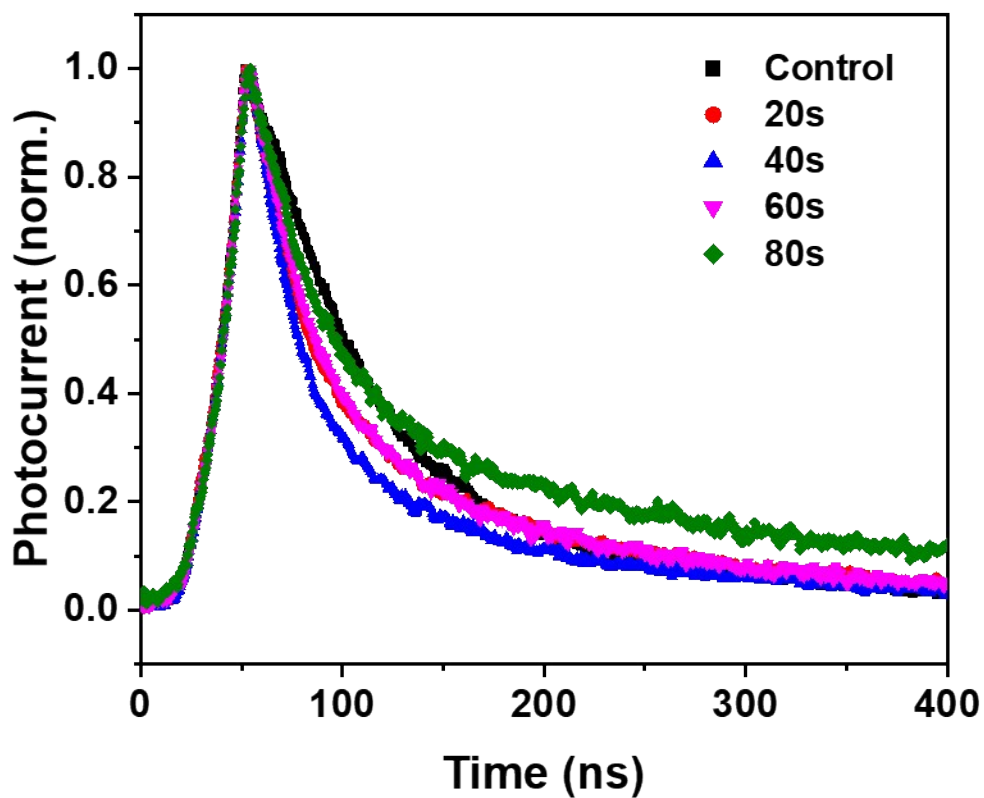


Figure S7. Transient photocurrent (bias = 0 V) decay traces of sequentially doped PBDBT:ITIC solar cells without MoOx under 488 nm excitation.

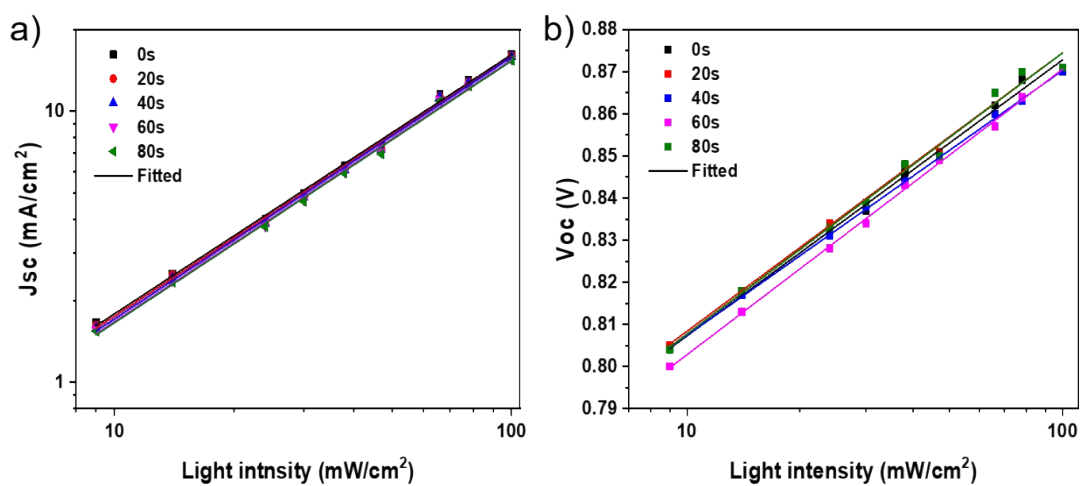


Figure S8. Short-current (J_{SC}) and open-circuit voltage (V_{OC}) versus light intensity characteristics.

Table S2. Extracted slopes of J_{SC} vs. P_{light} and V_{OC} vs. P_{light} characteristics.

Doping condition	Slope of J_{SC} vs. P_{light}	Slope of V_{OC} vs. P_{light} ($k_B T/q$)
0 s	0.956	1.109
20 s	0.958	1.119
40 s	0.966	1.065
60 s	0.966	1.130
80 s	0.966	1.148

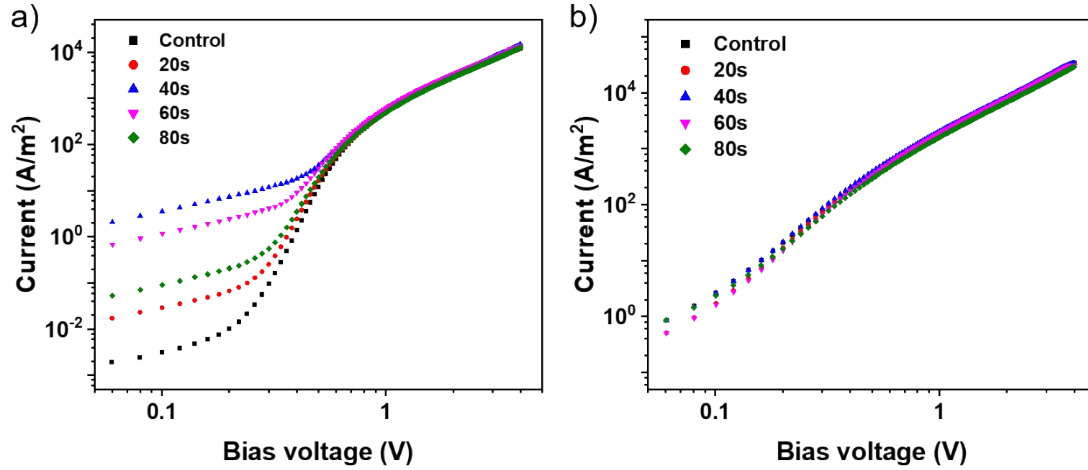


Figure S9. Dark J - V characteristics of (a) hole-only devices based on the structure of ITO/PEDOT:PSS/doped BHJ/Au and (b) electron-only devices based on the structure of ITO/ZnO/doped BHJ/ BCP/Al. The active layers are PBDB-T:ITIC blend films in different doping conditions.